Neurobiology of Disease 96 (2016) 335–345

Contents lists available at ScienceDirect

Neurobiology of Disease

journal homepage: www.elsevier.com/locate/ynbdi

Developing therapeutically more efficient Neurturin variants for treatment of Parkinson's disease

Pia Runeberg-Roos [a,*], Elisa Piccinini [a,1], Anna-Maija Penttinen [a,1], Kert Mätlik [a], Hanna Heikkinen [a], Satu Kuure [a,2], Maxim M. Bespalov [a,3], Johan Peränen [a,4], Enrique Garea-Rodríguez [b,5], Eberhard Fuchs [c], Mikko Airavaara [a], Nisse Kalkkinen [a], Richard Penn [d,6], Mart Saarma [a]

[a] Institute of Biotechnology, University of Helsinki, PB 56 (Viikinkaari 5D), FIN-00014, Finland
[b] Department of Neuroanatomy, Institute for Anatomy and Cell Biology, University of Freiburg, Freiburg, Germany
[c] German Primate Center, Göttingen, Germany
[d] CNS Therapeutics Inc., 332 Minnesota Street, Ste W1750, St. Paul, MN 55101, USA

ARTICLE INFO

Article history:
Received 26 May 2016
Revised 4 July 2016
Accepted 13 July 2016
Available online 15 July 2016

Keywords:
NRTN
Neurturin
GDNF
GFRα1
GFRα2
RET
Heparan sulfate
Heparin
Parkinson's disease
Growth factor

ABSTRACT

In Parkinson's disease midbrain dopaminergic neurons degenerate and die. Oral medications and deep brain stimulation can relieve the initial symptoms, but the disease continues to progress. Growth factors that might support the survival, enhance the activity, or even regenerate degenerating dopamine neurons have been tried with mixed results in patients. As growth factors do not pass the blood-brain barrier, they have to be delivered intracranially. Therefore their efficient diffusion in brain tissue is of crucial importance. To improve the diffusion of the growth factor neurturin (NRTN), we modified its capacity to attach to heparan sulfates in the extracellular matrix. We present four new, biologically fully active variants with reduced heparin binding. Two of these variants are more stable than WT NRTN *in vitro* and diffuse better in rat brains. We also show that one of the NRTN variants diffuses better than its close homolog GDNF in monkey brains. The variant with the highest stability and widest diffusion regenerates dopamine fibers and improves the conditions of rats in a 6-hydroxydopamine model of Parkinson's disease more potently than GDNF, which previously showed modest efficacy in clinical trials. The new NRTN variants may help solve the major problem of inadequate distribution of NRTN in human brain tissue.

1. Introduction

Parkinson's disease (PD) is a neurological disease in which midbrain dopaminergic neurons are lost. While the symptoms initially can be relieved by oral medications and later by deep brain stimulation, the dopaminergic neurons continue to degenerate in this chronic, progressive disease (Kordower and Björklund, 2013). Based on animal models, growth factors that support the survival or activity, or even restore the function of dopaminergic neurons have been regarded as candidates for a novel type of disease-modifying treatment. The Glial cell line-Derived Neurotrophic Factor (GDNF) (Lin et al., 1993) showed a strong potential in animal trials. However, although GDNF seemed beneficial in two open label clinical studies (Gill et al., 2003; Slevin et al., 2005), it failed in a double-blind study (Lang et al., 2006). More recently also neurturin (NRTN), a close homolog of GDNF (Kotzbauer et al., 1996) showed only limited effects in gene therapy-based Phase 2a and 2b clinical trials (Marks et al., 2010; Bartus and Johnson, 2016a; Bartus and Johnson, 2016b; Ceregene, Press release 21.5.2013). The reason why GDNF and NRTN work better in animal models than in the clinical trials is unclear (Bartus et al., 2013). GDNF and NRTN do not pass the blood-

Abbreviations: GDNF, Glial cell line-Derived Neurotrophic Factor; IHC, immunohistochemical; GAPDH, glyceraldehyde 3-phosphate dehydrogenase; GFRα1, GDNF family receptor α1; GFRα2, GDNF family receptor α2; IP, immunoprecipitated; MPTP, 1-methyl-4-phenyl-1,2,3,6-tetrahydropyridine; NRTN, neurturin; NV1–4, V5-tagged NRTN variants N1-4; N1–4, untagged NRTN variants; OHDA, hydroxydopamine; PD, Parkinson's disease; pgsA 745 cells, CHO cells deficient in heparan sulfate from ATCC; P-TYR, phosphotyrosine; RET, Rearranged during Transfection (a transmembrane tyrosine kinase receptor); SNpc, substantia nigra pars compacta; TH, tyrosine hydroxylase; WB, Western blotting.

* Corresponding author.
E-mail address: pia.runeberg@helsinki.fi (P. Runeberg-Roos).
[1] Equal second authors.
[2] Current address: Laboratory Animal Centre, University of Helsinki, Helsinki, Finland.
[3] Current address: University of Helsinki, Research Programs Unit, Molecular Neurology and Biomedicum Stem Cell Centre.
[4] Current address: University of Helsinki, Biomedicum, Department of Anatomy.
[5] Current address: Encepharm, Göttingen, Germany.
[6] Current address: NTF Therapeutics, Inc., 4950 S. Chicago Beach Dr., Chicago, IL 60615, USA.

Available online on ScienceDirect (www.sciencedirect.com).

http://dx.doi.org/10.1016/j.nbd.2016.07.008
0969-9961/

brain barrier and are delivered intraparenchymally. However, in the brain tissue their diffusion is hindered by their strong binding to extracellular matrix and cell surface heparan sulfated proteoglycans (Hamilton et al., 2001; Bespalov et al., 2011). Therefore promising results with these ligands in small rat brains (2 g), may not necessarily be directly applicable to the much larger human brain (1300 g). In primates an efficient intracranial diffusion of the growth factors is critically important. Monkeys with the largest distribution of GDNF recovered best from 1-methyl-4-phenyl-1,2,3,6-tetrahydropyridine (MPTP) lesions (Gash et al., 2005). Monkey studies with identical catheters and flow rates as in the unsuccessful clinical trial, suggested that the trial failed due to a poor and variable distribution of GDNF (Salvatore et al., 2006). Autopsies on patients receiving NRTN gene therapy showed that NRTN diffused <2 mm around the injection site (Bartus et al., 2011), and that an enigmatically sparse tyrosine hydroxylase (TH) response was achieved after the virus vector-driven NRTN delivery (Bartus and Johnson, 2016a). It is worth to keep in mind that NRTN easily aggregates at high concentration, therefore its limited diffusion cannot necessarily be compensated by a substantial increase of the dose. Here we developed biologically active NRTN variants with reduced binding to heparin and improved intracranial diffusion for treatment of PD.

2. Materials and methods

2.1. Modeling and cloning of NRTN and its variants

The 3D structure of NRTN was modeled based on the crystal structure of GDNF (Eigenbrot and Gerber, 1997; Parkash et al., 2008) using PyMol software (DeLano Scientific). For expression in mammalian cells, human NRTN (OpenBiosystems, BC137399) was subcloned (excluding the endogenous signal and prosequence) with an IgG signal sequence followed by the sequence of mature NRTN as previously described (Fjord-Larsen et al., 2005), except that pAAV-MCS (Stratagene) was used as a backbone. The variants were created by inverse PCR mutagenesis (primer sequences in the supplement) and all inserts were sequenced.

The V5-tag (GKPIPNPLLGLDST) was added to the N-terminus with the residues (AR) between the signal sequence and the V5 tag and (SG) between the V5-tag and the mature NRTN sequence. The cloning (primer sequences in the supplement) was done as above. The V5-tagged variants of human NRTN were named NV1-NV4. The cloning of NRTN for up-scaled expression is described below.

2.2. Expression, purification and characterization of NRTN

CHO cells were transiently transfected with GFP or the V5-tagged NRTN variants NV1-NV4 using Turbofect (Thermo Scientific). Two days later the media (DMEM, Sigma-Aldrich; 10% FBS, HyClone; 100 U/ml penicillin, Gibco; 100 μg/ml streptomycin, Gibco) were collected, boiled with reducing Laemmli buffer and analyzed by Western blotting with V5-antibodies (R960-25, Invitrogen).

NRTN production was up-scaled in CHO cells using constructs without the prosequence and tag-sequences with the proprietary QMCF Technology at Icosagen Ltd. (European Patent EP1851319). The NRTN variants were purified from the media by heparin affinity chromatography, GFRα2 affinity chromatography and gel filtration. The proteins were stored in 150 mM NaCl, 10 mM Na-citrate pH 5.0 at −20 °C (purification protocol in the Supplemental material). The N-terminal sequence of the purified NRTN variants was determined by Edman degradation using a Procise 494A HT Sequencer (Perkin Elmer/Applied Biosystems, Foster City, CA). The molecular mass of the proteins was determined using MALDI-TOF mass spectrometry (Ultraflex TOF/TOF, Bruker Daltonics). To increase the detection sensitivity in Western blots, untagged NRTN was analyzed under non-reducing conditions, without boiling with antibodies to NRTN (AF477, R&D Systems). Commercial NRTN and GDNF (from *E.coli*) were from Peprotech Inc. and ProSpec Ltd., respectively.

2.3. Heparin affinity chromatography

For initial screening, media from transiently transfected CHO cells were diluted with 10 mM HEPES, pH 7.2 and analyzed using heparin columns (Supplemental material). To characterize the affinity of the purified NRTN variants to heparin, we used a SMART System chromatograph (Pharmacia Biotech) equipped with a self-packed column (2 × 20 mm) with heparin Sepharose from HiTrap Heparin HP columns (GE Healthcare). The flow rate was 50 μl/min. After loading 2 μg of each purified NRTN variant to the column, the samples were eluted with a linear NaCl gradient (10 mM HEPES, pH 7.2, with NaCl up to 2 M). The elution was monitored by A214 nm and the corresponding salt concentration by measuring conductivity.

2.4. RET-phosphorylation and cell-based binding assays

Both assays were done as described in Supplemental material and (Virtanen et al., 2005). When purified NRTN variants, commercial NRTN or GDNF were used in RET-phosphorylation assays, they were diluted in DMEM. In cell-based binding assays competition of the ^{125}I-NRTN variants was performed with the unlabeled NRTN variants in DMEM with 0.5% BSA and 0.2% dry milk (containing soluble heparan sulfates). Monitoring of ^{125}I-NRTN was done either from cell lysates using a gamma counter (Perkin Elmer Wizard, 1480 automatic) or from intact cells using LigandTracer Grey (Ridgeview Instruments AB). In both cases IC_{50} was calculated based on 4–9 parallel data points with GraphPad Prism. Thereafter the mean IC_{50} was determined based on 2–5 independent measurements. As the concentration of ^{125}I-NRTN (50 pM) was much lower than the IC_{50} values obtained, the IC_{50} values correspond approximately to K_d (dissociation constant) values.

2.5. In vitro survival assay on embryonic dopaminergic neurons

Dissociated midbrain cultures from E13.5 NMRI mice were prepared (Planken et al., 2010), fixed at 5DIV and stained with anti-TH antibody (AB 1542, Millipore) and Cy3 affinity pure donkey anti-sheep IgG (713-165-147, Jackson). Quantification of TH-positive cells was done using images analyzed with Image-Pro Plus 5.1.2.59, with constant intensity and size range criteria throughout an experiment. The number of TH-positive cells for each data point was the average of at least 2 replicate micro islands. For inter-experiment normalization, this average was divided by the mean of all of the data points within the corresponding experiment. The resulting relative number of TH-positive cells in each experiment was used to calculate the average of all of the experiments (n = 3–8), finally expressed as per cent of the number of TH-positive cells surviving without added growth factors.

2.6. In vitro organ culture of kidney explants

E11.5 mouse urogenital blocks were dissected and cultured on Transwell filters (Fisher) in a Trowell-type system (Sainio et al., 1997) in DMEM medium (10% FCS, 1% Glutamax and 1% penicillin/streptomycin), supplemented with 500 ng/ml WT, NRTN variants N2 or N4. After 48 h, the explants were stained for calbindin D28K (sc-7691, Santa Cruz).

2.7. Immunocytochemical staining

NRTN variants were transiently expressed (2 days) in CHO cells. The media were stored at +4 °C. A second set of CHO cells was plated on uncoated cover-slips (2 days), transfected with GFRα2 (24 h) and exposed to the stored media containing the different NRTN variants. The cells were incubated with media for 10 min, rinsed with DMEM, fixed with

4% paraformaldehyde (PFA), permeabilized in 0.2% Triton X-100, blocked in 1% BSA and stained with V5-antibodies (R960-25, Invitrogen) and CY3-conjugated donkey anti-mouse antibodies (715.165.151, Jackson). For the second assay, with CHO cells and CHO cells deficient in heparan sulfate (pgsA 745 from ATCC), the cells were not permeabilized. The nuclei were stained with Hoechst (Invitrogen).

2.8. In vivo diffusion assays in rats

To characterize the diffusion of NRTN in the brain tissue of Wistar rats, each protein (5 μg in 10 μl) was injected using stereotactic surgery into the left striatum (AP +1.0, ML +2.8, DV −6.0, −5.5, −5.0 and −4.4 mm) as described below. After 24 h the rats were transcardially perfused with cold PBS and 4% PFA. The brains were removed and post-fixed in 4% PFA for 24 h. Following cryosectioning (40 μm) the slices were processed and stained with goat anti-NRTN antibodies (AF477, R&D Systems, 1:1000) (Voutilainen et al., 2009). For diffusion volume measurements, every sixth section was analyzed with the Cavalieri estimator function of the StereoInvestigator platform (MicroBrightField) attached to an Olympus BX51 microscope. The spacing of the grid was 250 μm.

2.9. In vivo assays in a rat 6-hydroxydopamine (6-OHDA) lesion model

All trials with male Wistar rats were carried out according to the laboratory animal care guidelines of the National Institute of Health, and were approved by the State Provincial Office of Southern Finland. Desipramine hydrochloride (15 mg/kg, Sigma-Aldrich) was administered intraperitoneally to the animals thirty minutes before 6-OHDA injection to protect the noradrenergic nerve terminals. The rats were anesthetized with isoflurane (Baxter), the left brain hemisphere was exposed through craniectomy and 7 μl of 6-OHDA (4 μg/μl, Sigma-Aldrich) was infused (0.5 μl/min), equally distributed between four sites into the striatum (AP +1.0, ML +2.8, DV −6.0, −5.5, −5.0 and −4.4 mm from scull). The needle was left in place for another 5 min before withdrawing. The hole in the skull was filled with bone wax (Surgical Specialties Corporation) and the wound was closed. Two weeks after the lesion, animals rotating ipsilaterally (see below) >220 times per 120 min were selected for stereotactic injection of the protein solutions (5 μg in 10 μl buffer) at a speed of 1 μl/min equally distributed between the identical four coordinates as above. The needle was withdrawn and the wound closed as above.

The rats were tested for amphetamine-induced rotation behavior (Kirik et al., 2000) 8 and 12 weeks after the lesion. Motor asymmetry was monitored in automated 25 rotometer bowls (Med Associates, Inc.) for 120 min after injection of amphetamine sulfate (2.5 mg/kg s.c. Sigma-Aldrich). The net rotation asymmetry score for each test was calculated by subtracting contralateral turns from ipsilateral turns to the lesion.

The forelimb use in spontaneous rearing was assessed using a cylinder test (Kirik et al., 2000) 6 and 10 weeks after the lesion. The rats were monitored for 5 min as they moved freely in the plexiglass cylinder (diameter 20 cm). The contacts made by each forepaw with the cage wall when rearing were scored by a blinded observer. The percentage of impaired forelimb contacts was calculated.

After 12 weeks the rats were transcardially perfused with saline and 4% PFA. The brains were cryosectioned (40 μm) and stained with biotinylated mouse anti-TH-antibodies (MAB318, Millipore). The number of TH-positive cells in the substantia nigra pars compacta (SNpc) and the optical density of the TH-positive fibers in the striatum were determined as previously described (Voutilainen et al., 2009). Cell numbers were counted using unbiased stereology and StereoInvestigator and are expressed for each animal as the mean cell numbers from 9 sections, percentage of the intact side. The fiber density was determined and presented as mean density (9 sections/brain), percentage of the intact side. The analyses were conducted in blinded manner by the experimenter.

2.10. In vivo diffusion assays in monkeys

Two cynomolgus monkeys (*Macaca fascicularis*) (from Covance Inc.) were implanted with bilateral intraputamenal catheters (Renishaw plc.) at Northern Biomedical Research. In total four catheters were allowed to heal in place for approximately 4 weeks, after which Magnevist® was administered for MRI-scanning (28-day intervals). On study day 90, the animals were administered Magnevist®, and then GFLs at a rate of 5 μl/min: N2 (170 μg at 1.0 μg/μl), N4 (170 μg at 0.83 μg/μl) and GDNF (225 μg at 1.0 μg/μl). The first animal received N4 in the left putamen and N2 in the right putamen; the second animal received GDNF in the left putamen. The infusion was followed by MRI. After necropsy, tissues were harvested and processed for IHC staining of GDNF (1:500, AB-212-NA, R&D Systems) and NRTN (1:200, AF477, R&D Systems) (Ai et al., 2003). Three marmoset monkeys (*Callithrix jacchus*) were bilaterally injected at Encepharm first with 5 μg of GDNF at 0.5 μg/μl (1 μl/min) to one side and then with 5 μg of N4 at 0.5 μg/μl (1 μl/min) to the other side. After necropsy, tissues were harvested, processed and stained for GDNF and NRTN as above. The monkey diffusion volumes were determined with the StereoInvestigator platform with sections 1 mm apart.

2.11. Expression analysis of NRTN receptors

The expression of GFRα1, GFRα2 and RET mRNAs in human brain tissues was analyzed by RT-PCR. Total RNA from human brain (Clontech) and poly(A)+ RNA from human substantia nigra, globus pallidus and putamen (T. Timmusk, Ethical Committee at Tallinn Technical University, (Timmusk et al., 1993) were used (1 μg) as templates for first-strand cDNA synthesis with RevertAid H Minus Reverse Transcriptase (Fermentas), using oligo(dT)$_{18}$-primers. RNA was substituted with water as a control (W1). For PCR, 10% of the synthesized cDNA was used as a template (primer sequences in the supplement). For each primer pair a water control substituting the cDNA (W2) was included. All the PCR reactions were performed using Phusion Hot Start II (Finnzymes/Thermo Scientific) with the manufacturer's 3-step protocol, 35 cycles. The annealing temperatures were 63 °C (GFRα1), 60 °C (GFRα2), 65 °C (RET) and 61 °C (GAPDH).

3. Results

3.1. Modeling and modifications of human NRTN

To design NRTN variants with lowered affinity to heparin, we started by predicting the location of putative heparin binding sites. The consensus sequences for heparin-binding are BBXB or BBBXXB (Cardin and Weintraub, 1989), where B is a basic amino acid and X is any residue. However, proteins lacking these consensus sequences may still bind to heparin (Delacoux et al., 2000). The initial analysis of the primary sequence of NRTN (Fig. 1) revealed a stretch of residues in the heel region (^{51}RRLRQRRRLRRER^{63}) which fits with the potential heparin-binding site criteria. Since heparin or heparan sulfates are linear polymers, the positively charged residues must be aligned in space. At least three residues should point in the same direction and be in close proximity to each other. To pinpoint the potential heparin-binding sites in NRTN which comply with this spatial rule we modeled the 3D structure of NRTN (Fig. 1) based on the known structure of GDNF (Eigenbrot and Gerber, 1997; Parkash et al., 2008). As the stretch of arginines (^{51}RRLRQRRRLRRER^{63}) is much longer than a single consensus sequence, and the area of positively charged arginines at the surface of NRTN is rather large, we substituted three amino acids (in variants N1 and N2) which were distributed over the surface of the protein. In variant N3 (five point mutations) we combined the mutations of N1 and N2, except that we restored the last arginine (RRLRQRRRLRRE**R**) which is conserved in NRTN, ARTN and PSPN. The other basic residues in this region are not conserved among the GFLs. PSPN does not bind

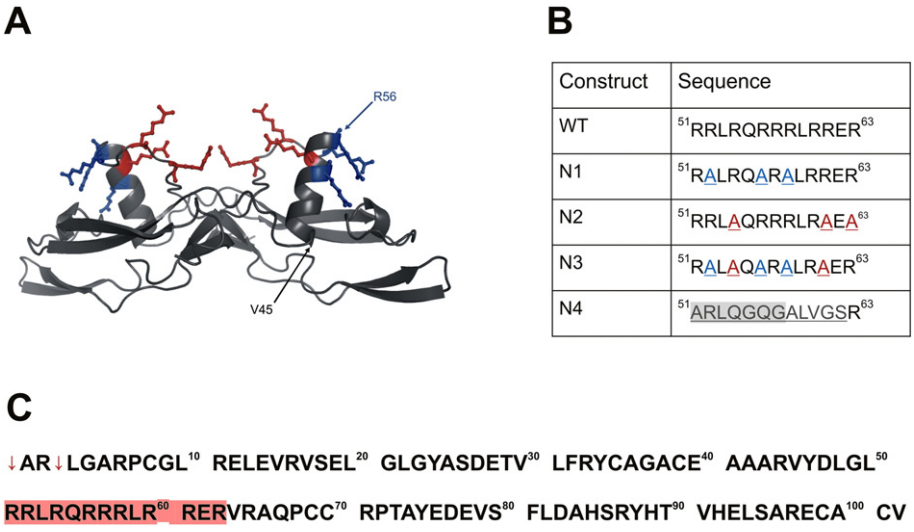

Fig. 1. Modeling of NRTN and design of new NRTN variants. (A) Model of NRTN, based on the crystal structure of GDNF. The beginning (V45) and end (R56) of the helix (heel) are shown with arrows. The location of mutated amino acids is shown in blue and red. (B) Overview of mutated amino acids in NRTN variants N1-N4. For N1-3 the mutated amino acids are shown in blue and red in accordance with (A), for N4 the sequence copied from PSPN is highlighted in gray, the other mutated residues are shown in gray without highlighting. (C) Primary structure of WT NRTN. Arrows indicate the location of two experimentally determined N-termini. The sequence shown in (B) is highlighted in red.

to heparin (Bespalov et al., 2011) and in variant N4 we therefore substituted for the heel region of NRTN the corresponding heel region of PSPN (ARLQGQG), and prolonged the sequence (ALVGS) to match the length of the original NRTN sequence (RRLRQRRRLRRE) (Fig. 1).

3.2. Initial screening for biologically active NRTN variants not binding to heparin

NRTN is homodimeric with a characteristic cysteine knot structure composed of seven disulfide bridges. Purification of over-expressed recombinant proteins with disulfide bridges from *E. coli* often requires harsh denaturation/renaturation and monomerization/dimerization procedures (Lin et al., 1993; Horger et al., 1998). NRTN produced in mammalian cells has a higher biological activity *in vitro* than NRTN expressed in *E. coli* (Hoane et al., 2000), maybe due to the stringent quality control of secreted proteins in mammalian cells. Therefore we expressed the NRTN variants in mammalian cells. As the secretion of NRTN from mammalian cells is impaired by the prosequence, we deleted it. We also replaced the endogenous ER-signal sequence with that of IgG and added a V5-tag to the N-terminus of the mature protein (Fjord-Larsen et al., 2005). All V5-tagged NRTN variants (NV1-NV4 and WT NRTN) were secreted from CHO cells. GDNF and NRTN bind to GDNF family co-receptors α1-2 (GFRα1-2) and activate the receptor tyrosine kinase RET. NRTN has a slightly higher affinity for GFRα2, while GDNF has a higher affinity for GFRα1 (Cik et al., 2000; Runeberg-Roos and Saarma, 2007). Our initial screening showed that the unpurified NRTN variants were active in RET-phosphorylation assays *in vitro* in the presence of either GFRα2 or GFRα1, and displayed decreased affinities for heparin (Fig. S1).

3.3. Proteolytic resistance of the NRTN variants

Unexpectedly, the concentration of the V5-tagged variants NV2 and especially NV4 was higher in the media of transiently transfected CHO cells than that of WT NRTN, NV1 and NV3 (Fig. S2). Similar results were obtained with ARPE-19 cells and with untagged NRTN variants from stably transfected CHO suspension cells. We found that the increased concentrations of NV2 and NV4 are not explainable by differential protein secretion or adhesion. As WT NRTN and NV2 are more sensitive to proteolytic degradation than NV4, an improved resistance to proteolytic degradation may at least partly explain the result (Fig. S2).

3.4. Purification and characterization of the NRTN variants

The expression of all NRTN variants was up-scaled in CHO suspension culture cells. Neither the prosequence nor the V5-tag was included in the final expression constructs. The untagged variants are called N1-N4. Normally gel filtration, cation exchange and heparin columns are used for the purification of GFLs (Lin et al., 1993; Horger et al., 1998). Since the NRTN variants have very different heparin affinities and pI values (WT: pI 9.01, N1: pI 8.27, N2: pI 8.27, N3: pI 7.01, N4: pI 6.33), we purified all NRTN variants based on their affinity to GFRα2. The approximate yields per ml of media were: 0.4 μg WT, 0.6 μg N1, 2.0 μg N2, 3.4 μg N3, 7.5 μg N4. The purity of the proteins was verified on non-reducing SDS-PAGE stained with Coomassie Brilliant Blue (Fig. 2).

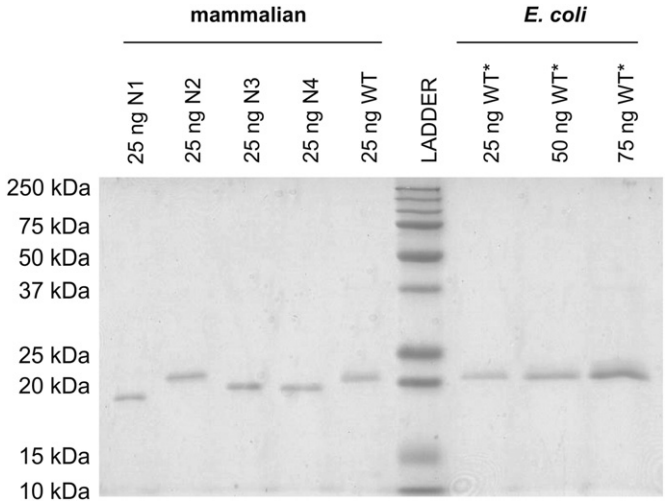

Fig. 2. Quantification of the purified untagged NRTN variants. Equal amounts of the purified NRTN variants were compared to each other and to commercial NRTN from *E. coli* on a 15% SDS-PAGE, stained with Coomassie brilliant blue.

Direct N-terminal sequencing of the purified protein preparations identified the expected N-terminal sequence ↓ARLGARP… in all of the NRTN variants (Fig. 1). In addition, a very small portion of WT and N2 was cleaved two amino acids after the expected cleavage site (AR↓-LGARP…), similar to an additional cleavage site in GDNF (Piccinini et al., 2013). These additional cleavage sites are important to take into account when designing assays with N-terminally tagged GFLs. Mass spectrometry verified the molecular mass of the purified NRTN variants to correspond to the expected theoretical mass of single protonated dimers without prominent posttranslational modifications (theoretical mass/determined mass in Da, WT: 23,355/23,345, N1: 22,844/22,807, N2: 22,844/22,822, N3: 22,504/22,469, N4: 22,165/22,143). Based on these assays we considered the quality of the proteins suitable for functional testing.

3.5. Stability of the purified proteins

When the purified NRTN variants N2, N3, N4 and WT NRTN were incubated at 37 °C at low concentration they were fully stable for four weeks (described in Supplemental material and Fig. S3). However, WT NRTN, N3 and especially N1 showed a strong tendency to precipitate during concentration, purification and biochemical assays. Therefore we focused on N2 and N4 which give better yields, are more stable and easier to handle.

3.6. Decreased affinity of the purified NRTN variants to heparin

The heparin binding capacity of the purified untagged NRTN variants was determined by heparin affinity chromatography. Commercial WT NRTN eluted with a peak at 1.07 M NaCl, WT NRTN from CHO cells eluted at 1.08 M NaCl and the NRTN variants at significantly lower NaCl concentrations: 0.97 M (N1), 0.56 M (N2), 0.56 M (N3) and 0.48 M (N4) (Fig. 3). These results are in full accordance with the initial screening of the V5-tagged unpurified NRTN variants (Fig. S1). An example of the technical difficulties with N1 is shown in Fig. 3: although the amount of loaded N1 equaled that of the other NRTN variants, the protein was hardly detectable after elution. ARTN, NRTN and GDNF elute with peaks of around 1.3 M, 1.1 M and 0.9 M NaCl respectively (Alfano et al., 2007), while PSPN elutes with 0.5 M NaCl (Bespalov et al., 2011). Therefore N2 and N4 are new GFL variants with exceptionally low affinities for heparin.

3.7. Biological activity of the purified NRTN variants in vitro

Due to NRTN aggregation and adhesion, we used affinity chromatography and ^{125}I-NRTN binding to cells instead of Biacore assays for ligand-receptor affinity studies. In line with results on WT NRTN (Cik et al., 2000), all NRTN variants bind more strongly to GFRα2 than to GFRα1. Furthermore, under stringent affinity chromatography conditions, in the absence of RET, the binding of the new NRTN variants to both GFRα1 and GFRα2 receptors is slightly weaker than that of WT NRTN (Fig. S4). The heel region is not directly involved in interactions with the GFRα receptor in either ARTN or GDNF (Parkash et al., 2008). Therefore this region was predicted to be optimal for making mutations which affect the binding of NRTN to heparin but not to GFRα2. The mutations in the helix region might have a slight effect on the orientation of the receptor-binding finger-like structures in NRTN (Fig. 1).

The presence of RET is known to stabilize the binding of GDNF to the receptor complex (Virtanen et al., 2005). In binding assays on CHO cells expressing GFRα2, RET and heparan sulfates, the mean IC_{50} value was 5.9 nM for WT NRTN from mammalian cells (n = 5), when measured from cell lysates after competition with commercially available WT NRTN from *E. coli*. When using intact cells, ^{125}I-NRTN variants from mammalian cells and homologous competition, the mean IC_{50} values were 4.65 nM for WT NRTN (n = 2), 3.13 nM for N2 (n = 3) and 1.42 nM for N4 (n = 4) (Fig. 4A), showing that in the presence of RET, WT NRTN, N2 and N4 have a similar affinity to the GFRα2/RET receptor complex.

To study whether the NRTN variants have the same capacity to activate RET as WT NRTN, we performed dose-dependent RET-phosphorylation assays. Based on two/three repetitions of the assays we conclude that when the purified proteins are applied in cell culture media onto fibroblasts transfected with either GFRα2 or GFRα1, all NRTN variants can activate RET in a similar dose-dependent manner (Fig. 4B).

Next we compared the biological activity of WT NRTN and the variants N2 and N4, in an *in vitro* survival assay on dopaminergic neurons from dissociated mouse midbrains (E13.5), which express GFRα1 (but not GFRα2) and RET (Cacalano et al., 1998), and

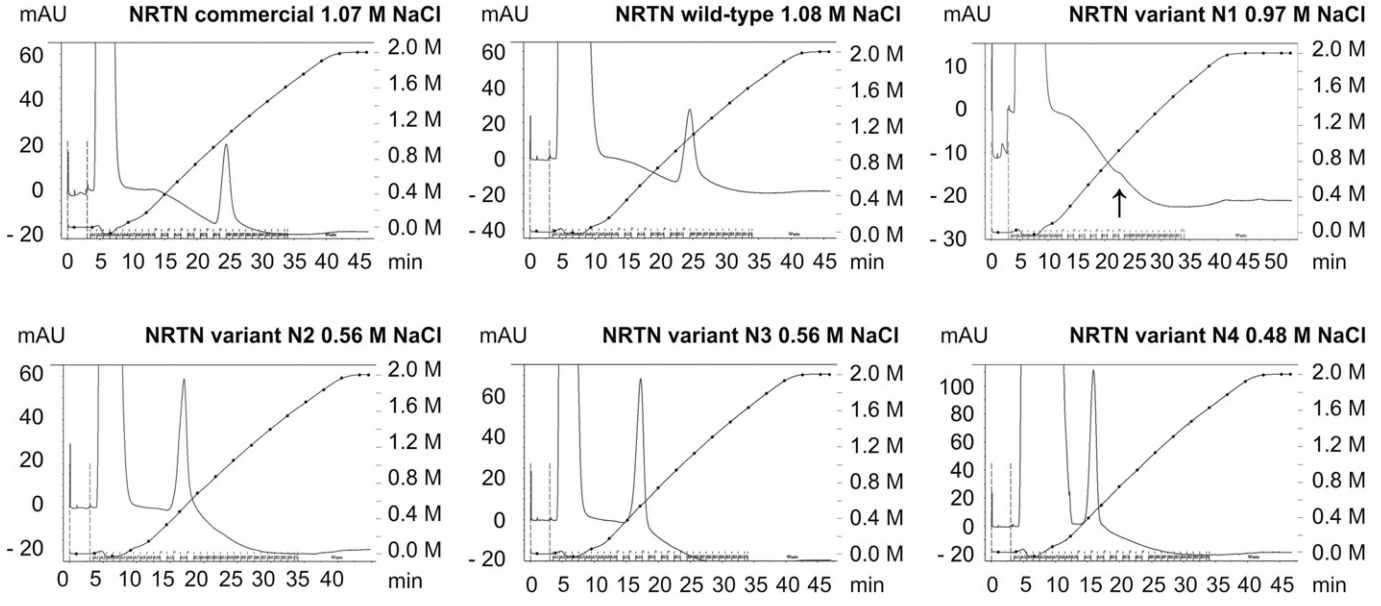

Fig. 3. Heparin affinity chromatography analysis of purified, untagged NRTN variants. The purity of the proteins was verified by SDS-PAGE, and further characterized by N-terminal sequencing and mass spectrometric analyses. Thereafter the proteins were loaded on heparin affinity chromatography column from which they were eluted with a linear NaCl gradient (right axis). The elution of the proteins was monitored by their absorption at 214 nm (left axis). The salt concentration at the elution peaks is shown for each protein. For N1 the peak is indicated with an arrow (↑).

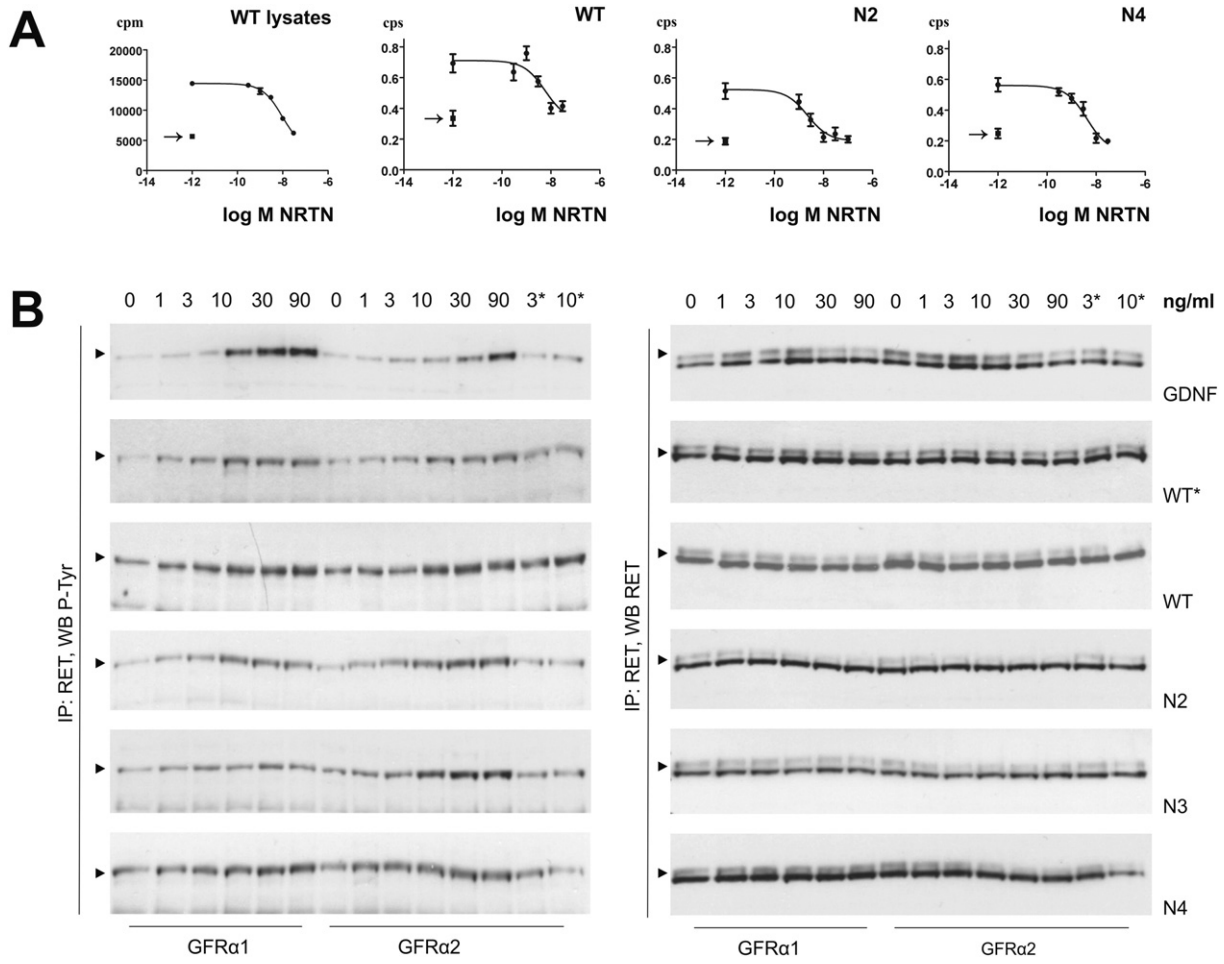

Fig. 4. Receptor activating capacity of the purified untagged NRTN variants. (A) Examples of cell-based binding assay on CHO cells transfected with GFRα2 and RET. Iodinated WT NRTN, N2 or N4 was added to the cells in the presence of increasing concentrations of the corresponding unlabeled NRTN variant. The background (→) was in each case determined on CHO cells transfected with GFP and RET. ^{125}I was monitored as counts per minute (cpm) from cell lysates or counts per second cells (cps) from intact cells. The number of parallel data points used to plot each graph is 4 for WT when measured from cell lysates and at least 7 for WT/N2/N4 when measured on intact cells. Error bars indicate SEM. For IC_{50} calculations each experiment was repeated 2–5 independent times. (B) Dose-dependent RET-phosphorylation assays. The purified NRTN variants (N2-N4, WT), commercial NRTN from *E. coli* (WT*) or GDNF (1–90 ng/ml) were used to stimulate MG87-RET cells transiently transfected with either GFRα1 or GFRα2. WT* was used for normalization at 3 and 10 ng/ml (3* and 10*). The immunoprecipitates were analyzed after Western blotting, with antibodies to phosphotyrosine (P-Tyr, left) and RET (right). The cell surface-located form of RET (170 kDa) is indicated with an arrowhead (►).

probably also heparan sulfates. Also in this dose-dependent survival assay N2, N4 and WT NRTN exhibited similar activity (one-way ANOVA, Tukey's *post hoc* test for differences between treatment and control) (Fig. 5A).

To compare the biological activity of the NRTN variants in tissue, we used mouse embryonic kidney cultures. GDNF induces extra ureteric budding and swelling of the definitive ureteric tips when added to kidney cultures (Sainio et al., 1997). However, although NRTN induces ureteric branching in organ cultures, it appears unable to induce ectopic buds (Davies et al., 1999). Accordingly, under our experimental conditions WT NRTN (from both *E. coli* and mammalian cells) failed to induce ectopic ureteric budding even at 500 ng/ml. Interestingly, both N2 and N4 induced ectopic ureteric buds and swelling of the definitive buds. The stronger activity of N2 and N4 correlates with a higher stability of these proteins in the media of the kidney cultures (Fig. 5B), and possibly with a better diffusion in the tissue. It should be noted that N2 and N4 also showed an improved stability in the cell culture media of mammalian cell lines (Fig. S2).

The affinity of the NRTN variants to GFRα2 enabled a purification method based on GFRα2-affinity chromatography. The biological activity of the purified NRTN variants was furthermore verified with binding assays, dose dependent RET-phosphorylation assays, *in vitro* survival assays and kidney *in vitro* organogenesis assays. We conclude that the mutations in the heel region affect the structure of NRTN only slightly, without impairing its biological activity.

3.8. Attachment to the cell surface and diffusion of the NRTN variants in the rat brain

GDNF, NRTN and ARTN attach to cells either by binding to GFRα or to heparan sulfated proteoglycans (Bespalov et al., 2011). Here we show that while WT NRTN attaches to the cell surface of CHO cells lacking GFRα receptors, N4 does not. When the cells are transfected with plasmids encoding GFRα2 receptors, both ligands attach to the cell surface (Fig. 6A). When CHO pgsA 745 cells, lacking heparan sulfates (deficient in xylosyltransferase and unable to initiate glycosaminoglycan synthesis), were used in the same type of experiments, neither ligand attached to the cell surface in the absence of GFRα2 (Fig. 6B).

In vivo the affinity of GFLs to extracellular heparan sulfates depends on the precisely regulated biochemical modification of these carbohydrates (Bespalov et al., 2011; Rickard et al., 2003). Immunohistochemical staining of rat brains 24 h after injection of the proteins (5 μg), shows that N2 (126 mm^3) and N4 (217 mm^3) diffused better than commercial WT NRTN (57 mm^3) (Fig. 6C–D). Although binding of NRTN to heparan sulfates could mediate protection from proteolysis and extracellular stability (Rickard et al., 2003), N2 and N4 show an improved resistance to

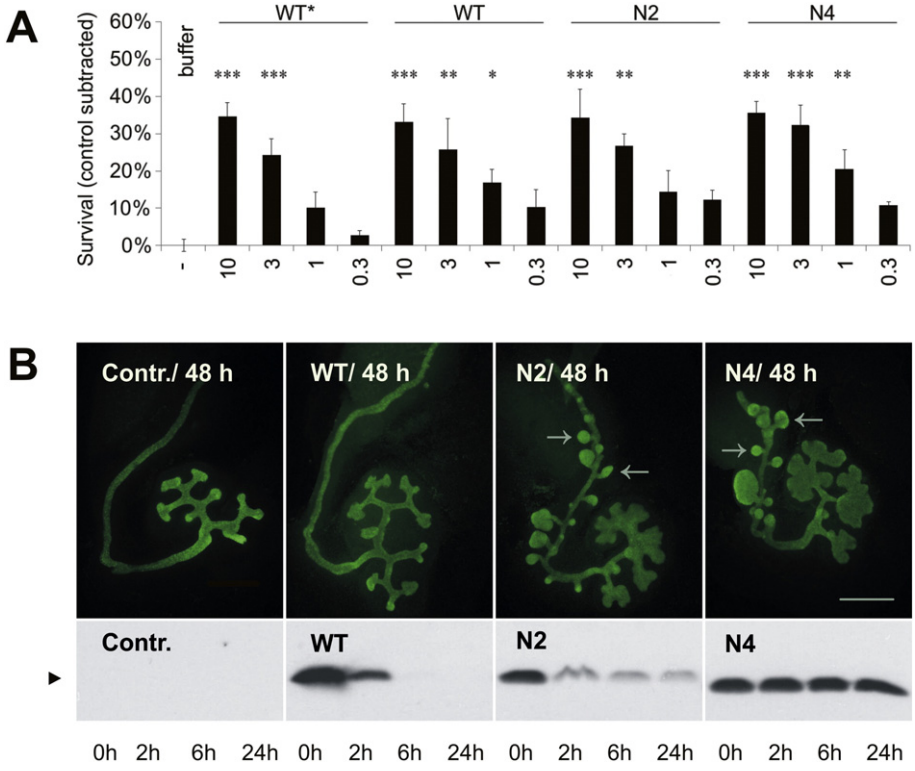

Fig. 5. *In vitro* activity assays using purified untagged NRTN variants (A) *In vitro* survival assay on embryonic dopaminergic neurons. Tyrosine hydroxylase positive cells were counted after survival induction with NRTN variants (N2, N4, WT) and commercial NRTN from *E. coli* (WT*) at 0.3–10 ng/ml. The number of tyrosine hydroxylase positive cells in the absence of ligands (buffer) was used as a control (100% survival). The results are shown after subtraction of this baseline (100%) control. Each experiment was done using two replicate micro islands and was repeated 3–8 independent times. Error bars indicate SEM., $p < 0.05$ (*), $p < 0.01$ (**), $p < 0.001$ (***). (B) Embryonic kidney organogenesis assay. Kidney explants were incubated with purified N2, N4 or WT NRTN (500 ng/ml) for 48 h and stained with anti-calbindin antibodies. Scale bar 200 μm. Explants incubated without added ligands were used as a control (Contr.). Under each kidney explant is a Western blot analysis of the amount of NRTN in the media at 0, 2, 6 or 24 h. Please note that the antibody to NRTN recognizes dimeric WT NRTN about fivefold more efficiently than N2 and N4 (see Fig. 6E). The arrowhead (►) indicates 20 kDa.

proteolytic cleavage *in vitro* (Fig. 5B, S1) and are detectable by immunohistochemical staining 24 h after injection into rat brains (Fig. 6C). The weaker staining of N4 could be due to the dilution factor and the affinity of the anti-NRTN antibody: in Western blots the affinity of this antibody is significantly lower for N2 and N4 than for WT NRTN (Fig. 6E).

3.9. Biological activity of N2 and N4 in a rat 6-OHDA model of PD

The neurorestorative activity of the NRTN variants *in vivo* was tested in a rat 6-OHDA model of PD (Kirik et al., 2000). Traditionally high doses of GFLs are used in rat models of PD (up to 100 μg). To distinguish between the effects of the different proteins, we used a severe lesion (28 μg 6-OHDA intrastriatally) and a relatively low dose of the proteins (5 μg, injected intrastriatally two weeks after the lesion) (Fig. 7A). In these experiments the injection volume is a limiting factor (10 μl). Since WT NRTN precipitated at concentrations above 0.1 μg/μl we were unable to include it in this set-up. N2 and N4 were compared to the vehicle and to commercial GDNF from *E. coli* (used in clinical trials, and considered as gold standard in animal models).

As a behavioral read-out of the unilateral dopamine deficits we used amphetamine-induced rotation assays and a non-pharmacological cylinder tests. Analysis (repeated measures ANOVA) of the results from the rotation assays revealed significant drug treatment effects ($F_{3,40} = 3.2$, $p = 0.033$). The Fisher PLSD *post hoc* test showed significant differences between the vehicle- and N4-treated rats ($p < 0.01$), between N2- and N4-treated rats ($p < 0.05$) and between GDNF- and N4-treated rats ($p < 0.05$) (Fig. 7B). Statistical analysis (Kruskal-Wallis non-parametric ANOVA) of the results from the cylinder test also revealed a significant drug treatment effect after ten weeks ($p = 0.0138$). The Dunn's Multiple comparison test showed a significant difference between the vehicle- and N4-treated groups ($p < 0.05$) (Fig. 7C), but not for GDNF.

TH-positive cells in the substantia nigra and TH-positive fibers in the striatum were quantified after the rotation assay at twelve weeks. Statistical analysis (one-way ANOVA) of the number of TH-positive cells in substantia nigra revealed significant drug treatment effects ($F_{3,40} = 2.951$, $p = 0.0441$). *Post hoc* analysis with Fisher's PLSD test showed a significant difference between all treated groups and the vehicle group ($p < 0.05$) (Fig. 7D). Statistical analysis of TH-positive neurites in the striatum, (one-way ANOVA), also revealed significant drug treatment effects ($F_{3,40} = 4.24$, $p = 0.011$). The Fisher PLSD *post hoc* test showed significant differences between vehicle- and N4-treated rats ($p < 0.01$), N2- and N4-treated rats ($p < 0.01$), as well as GDNF- and N4-treated rats ($p < 0.05$) (Fig. 7E), but not between vehicle and GDNF.

Our results with read-outs from four independent methods (cylinder test, amphetamine induced rotation, number of TH-positive cell somas in substantia nigra and fiber density in the striatum), at different time points are coherent, and show that mammalian N4 improves the conditions of the 6-OHDA lesioned animals, better than GDNF from *E. coli*. It should be noted that N4 improved the conditions of the rats in spite of its small dose (5 μg) in severely lesioned rats (28 μg 6-OHDA).

3.10. Diffusion of N2 and N4 in non-human primate brains

Equimolar amounts of GDNF (225 μg/225 μl), N2 (170 μg/170 μl) and N4 (170 μg/205 μl) were infused into the putamen of cynomolgus monkey brains (n = 1). Immunohistochemical staining shows that

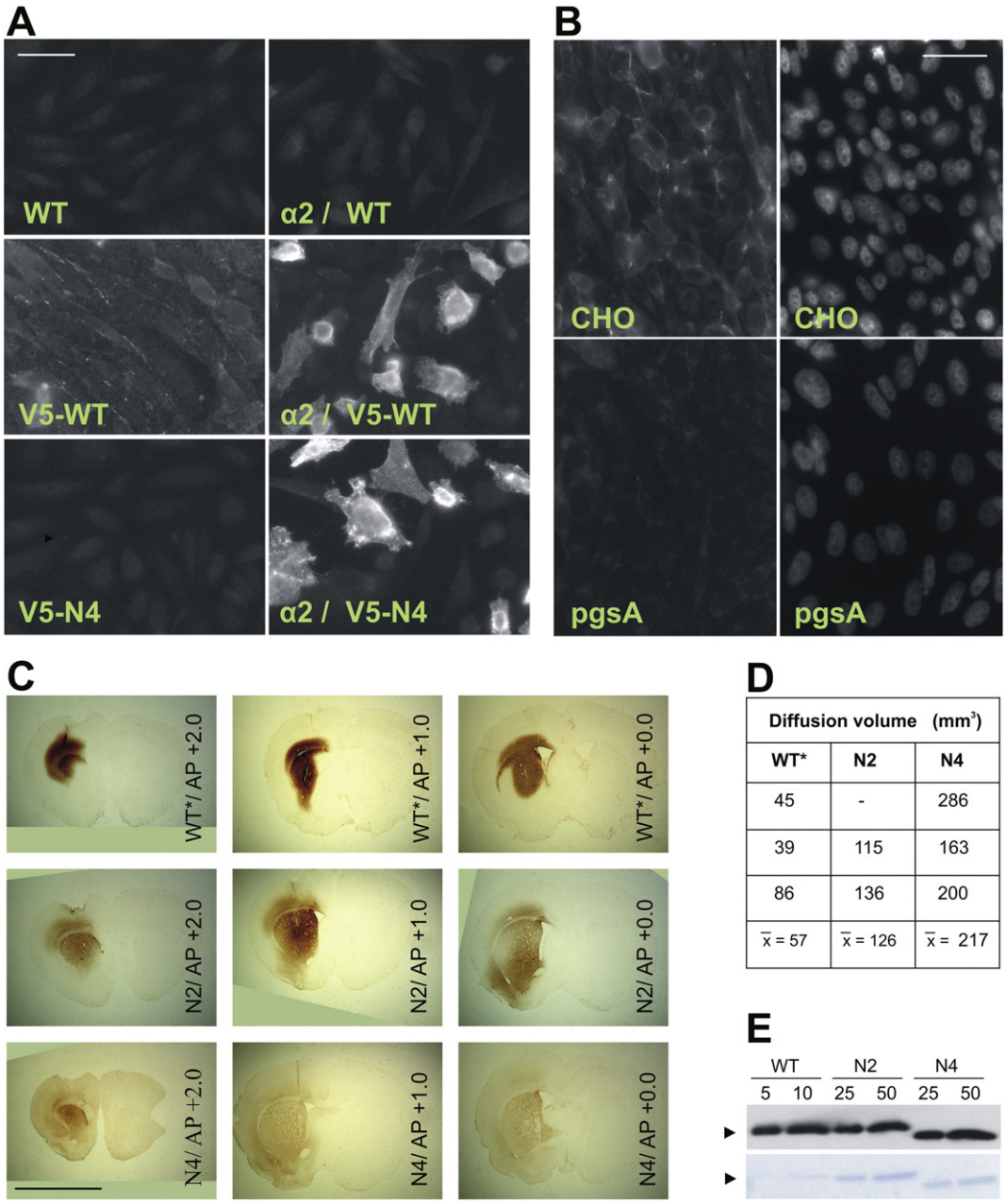

Fig. 6. Attachment to the cell surface and diffusion of the NRTN variants in rat brains. (A) Binding of NRTN variants to CHO cells. Untransfected cells (left) and GFRα2-transfected cells (α2) (right) were incubated with untagged WT NRTN (WT), V5-tagged WT NRTN (V5-WT) or V5-tagged N4 (V5-N4) and stained with antibodies to V5. Scale bar 30 μm. (B) Binding of NRTN to CHO cells with an intact or defective synthesis of glycosaminoglycans. Untransfected CHO (CHO) or pgsA-745 (pgsA) cells were incubated with V5-tagged WT NRTN and stained with antibodies to V5 (left) and Hoechst to visualize the nuclei (right). Scale bar 30 μm. (C) Diffusion of the NRTN variants in the rat brain. The untagged NRTN variants N2 and N4 as well as commercial NRTN from *E. coli* (WT*) (5 μg) were unilaterally injected into the striatum and detected by IHC. The panels in the middle represent sections at the injection site (AP +1.0). Sections 1 mm apart from the injection site are shown to the left (AP +2.0) and right (AP +0.0). Scale bar 7 mm. (D) Overview of the total diffusion volumes of WT*, N2 and N4 in all analyzed rats. (E) Characterization of the affinity of the antibodies to NRTN. WT NRTN (5, 10 ng), N2 (25, 50 ng) and N4 (25, 50 ng) were analyzed by Western blotting with antibodies to NRTN (upper panel) or stained with Coomassie brilliant blue (lower panel), the arrowhead (►) indicates 20 kDa.

GDNF (619 mm^3) and N2 (538 mm^3) diffused approximately over the same volume although N2 was applied in a 25% smaller infusion volume. N4 (1228 mm^3) diffused over the biggest volume (Fig. S5). Immunohistochemical staining of marmoset monkey brains (n = 3) 8 h after injection of the proteins (5 μg), shows that N4 (106.1 mm^3) diffuses significantly better ($p = 0.018$) than commercial GDNF (18.4 mm^3) (Fig. 8A, S6). Taken together our results show that especially N4 has a decreased affinity to heparin (Figs. S1C, 3), and to heparan sulfated proteoglycans on the cell surface/extracellular matrix *in vitro* (Fig. 6A–B). NRTN variant N4 also displays an improved diffusion in rat and monkey brain tissues *in vivo* (Fig. 6C–D, 8A–B, S5, S6).

3.11. Expression of N2 and N4 receptors in human basal ganglia

It is worth to note that both N2 and N4 are active in mouse embryonic dissociated midbrain cultures, as well as in mouse kidney organogenesis assays, although GFRα2 is lacking from these tissues (Cacalano et al., 1998; Golden et al., 1999).These assays show that the biological activity of N2 and N4 can be mediated not only by GFRα2/RET but also GFRα1/RET. Successful clinical use of NRTN depends on the expression of the signal transducing receptors in the target tissues. The expression of GFRα1 and RET has previously been detected by quantitative real-time RT-PCR in the putamen of elderly humans, with no significant

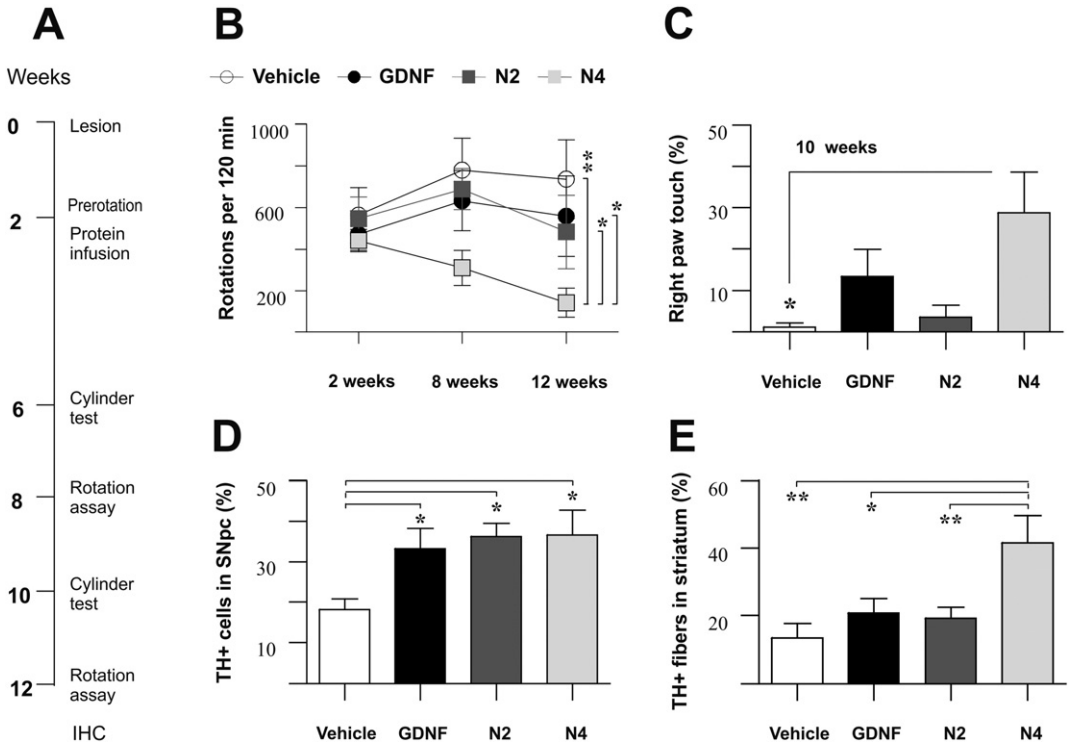

Fig. 7. *In vivo* assays in a rat 6-OHDA lesion model. (A) Schema of the assay. After the 6-OHDA lesion (2 weeks), 5 μg of commercial GDNF, N2 or N4 were injected unilaterally into the striatum. The rats (vehicle: n = 9, GDNF: n = 10, N2: n = 12, N4: n = 13) were characterized by (B) amphetamine-induced rotation assays at weeks 8 and 12, (C) cylinder tests at week 10, (D) IHC estimation of TH-positive cell somas in SNpc at 12 weeks, (E) IHC quantification of TH-positive fiber density in the striatum at 12 weeks, significant difference to vehicle, $p < 0.05$ (*), $p < 0.01$ (**).

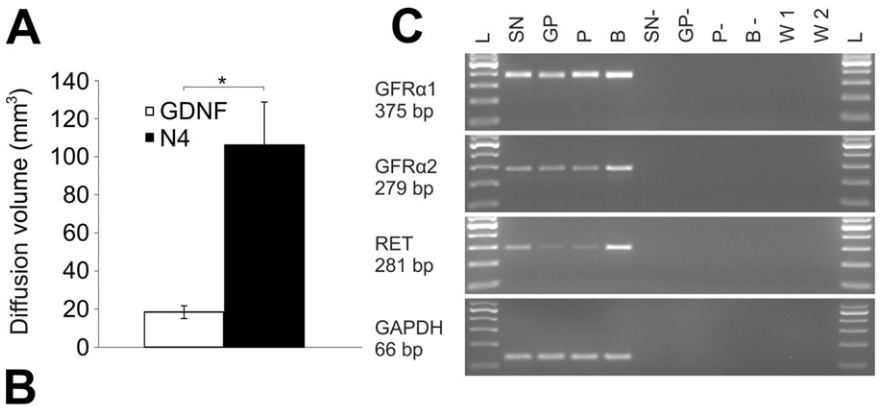

B

Species and conditions	Diffusion ratio (mm³/μg protein)			
	GDNF	WT NRTN	N2	N4
Rat (n = 3), 24 h 5 μg/10 μl in 4 sites 1 μl/min over 10 min		11.4	25.2	43.4
Cynomologous monkey (n = 1), 2h 170-225 μg/170-225 μl by catheter 5 μl/min over 35-45 min	2.75		3.2	7.2
Marmoset monkey (n = 3), 8 h 5 μg/10 μl in 1 site 1 μl/min over 10 min	3.7			21.2

Fig. 8. Diffusion of the NRTN variants in rat and monkey brains and expression analysis of the receptors in human brains (A) Volume measurements show a significantly ($p = 0.018$) improved diffusion of N4 compared to GDNF in marmoset monkey brains (n = 3), see Fig. S6 for an overview of all sections used for the volume estimations. (B) Comparison of the spreading of N4 compared to N2, WT NRTN or GDNF in rat brains, n = 3, diffusion time 24 h (see Fig. 6C-D), cynomolgus monkey brains, n = 1, diffusion time 2 h (see Fig. S5) and marmoset monkey brains, n = 3, diffusion time 8 h (see Fig. S6). A summary of the experimental parameters is given to the left. (C) RT-PCR analysis of mRNA encoding GFRα1, GFRα2 and RET in human basal ganglia. GAPDH was included for normalization. RNAs were from substantia nigra (SN), globus pallidus (GP), putamen (P) and whole brain (B). Samples incubated without reverse transcriptase are marked with a minus, W 1 and W 2 are water controls described in the materials and methods. The ladder (L) used for GFRα1/2 and RET is from the bottom 100, 200, 300, 400, 500, 600 bp and for GAPDH 50, 100, 150, 200, 250, 300 bp.

changes in patients with PD (Bäckman et al., 2006). Since it was unclear whether GFRα2 is expressed in human midbrain we performed RT-PCR analysis of adult human tissues. Our results show that mRNAs of GFRα2, GFRα1 and RET are expressed in human substantia nigra, globus pallidus and putamen (Fig. 8C).

4. Discussion

GDNF and NRTN have given modest and controversial results in PD clinical trials (Lang et al., 2006; Marks et al., 2010; Bartus and Johnson, 2016a; Bartus and Johnson, 2016b; Bartus et al., 2011, Ceregene, Press release 21.5.2013). Controversy surrounds the intraparenchymal infusions of GDNF protein (produced in *E. coli*) with the first studies reporting significant improvement in motor function but the blinded phase II trials failing to do so. Non-human primate studies have shown marked variability of GDNF distribution when infused in the same way as in the phase II study, and motor improvement was only seen in animals with the widest GDNF distribution. Gene therapy-based clinical trials with NRTN have not achieved their primary endpoint of motor improvement. Autopsy showed only modest changes in TH-positive cell numbers and very limited NRTN distribution around the injection sites. Consideration of the poor and variable distribution led us to create better diffusing NRTN variants with a decreased affinity to heparan sulfates in the extracellular matrix and on the cell surface. We validated the improved spreading of these variants in brain tissue of rats, cynomolgus and marmoset monkeys.

The molecular properties of NRTN are important to take into account in PD clinical trials. It is well established that low concentrations of GFLs (10 ng/ml) trigger RET activation *in vitro*. According to these results, 80 ng would be enough so to cover the two-sided human putamen, which has a volume of <8 ml (Yin et al., 2009). Instead intriguingly high doses of 3–43 μg/day (Gill et al., 2003; Slevin et al., 2005; Lang et al., 2006) have been used in clinical trials. It could be that some protein chemical properties of GFLs have necessitated the use of excessive *in vivo* doses. NRTN is very prone to precipitate at increased protein concentration (above 0.1 μg/μl) and upon buffer exchange. Therefore the transition of high amounts of NRTN from the injection buffer to the tissue implies high precipitation risks for this protein. Inside the tissue the diffusion of NRTN is severely hampered by its high affinity to heparan sulfates. Here we modified NRTN with the intention to decrease its affinity to heparan sulfates. This modification turned out to improve also the stability of the protein and facilitate its handling. To optimize protein folding and dimerization, both important for receptor activation, we used a mammalian expression system for production of the mutants. Taken together, improved chemical properties of NRTN are highly relevant for therapeutic efficacy and success in clinical trials.

5. Conclusions

For treating patients with Parkinson's disease, we designed and characterized NRTN variants with an increased diffusion. The improved diffusion of these novel NRTN variants is particularly relevant in humans, with brains about six hundred times bigger than those in rats. In our rat 6-OHDA model of PD the NRTN variant N4 shows a clear improvement in motor function and protects and repairs dopamine neurons *in vivo* more efficiently than GDNF from *E. coli*. This may not be due only to an improved diffusion, but also to an increased proteolytic stability. For these reasons the NRTN variants N2 and N4 are good candidates for the treatment of PD and are currently being tested in non-human primate models of PD. Whether our newly created neurotrophic factor variants with improved diffusion and stability will slow or reverse the degenerative process of PD will have to await human trials.

Conflict of interest

RP was a founder and shareholder of CNS Therapeutics, Inc. PRR, MB, RP and MS are inventors on the patent *Improved neurturin molecules* - US Patent 8445432, May 2013, owned by NTF Therapeutics, Inc.

Acknowledgments

We thank Heidi Virtanen for cloning assistance; Maria Lindahl for the human GFRα2 clone; Tõnis Timmusk for the human RNA samples; Susanne Bäck for her help with the IHC staining; Ridgeview Instruments AB for trial-use of LigandTracer Grey; Northern Biomedical Research Inc.; Yi Ai and Don Gash for the cynomolgus monkey infusion experiments; Christina Schlumbohm and Gabriele Flügge for marmoset monkey infusion experiments. This work was supported by CNS Therapeutics, Inc., the S. Jusélius Foundation (MS) Academy of Finland #250275, #256398, #281394 (MA, AMP). EP (Integrative Life Science doctoral programme) was supported by the University of Helsinki Research Foundation and CIMO, Finnish Government Scholarship Pool. HH, PRR, EP, AMP, KM, SK, MMB, JP, EGR, EF, MA, NK, MS designed and performed experiments. HH, PRR, EP, AMP, KM, SK, MMB, MA, NK, RP, MS analyzed data. PRR, EP, AMP, KM, SK, MA, RP, MS wrote the paper or sections of it. PRR, RP, MS directed the studies. All authors commented on the manuscript.

Supplementary data

Supplementary data to this article can be found online at http://dx.doi.org/10.1016/j.nbd.2016.07.008.

References

Ai, Y., Markesbery, W., Zhang, Z., Grondin, R., Elseberry, D., Gerhardt, G.A., Gash, D.M., 2003. Intraputamenal infusion of GDNF in aged rhesus monkeys: distribution and dopaminergic effects. J. Comp. Neurol. 461, 250–261.

Alfano, I.P., Vora, P., Mummery, R.S., Mulloy, B., Rider, C.C., 2007. The major determinant of the heparin binding of glial cell-line-derived neurotrophic factor is near the N-terminus and is dispensable for receptor binding. Biochem. J. 404, 131–140.

Bäckman, C.M., Shan, L., Zhang, Y.J., Hoffer, B.J., Leonard, S., Troncoso, J.C., Vonsatel, P., Tomac, A.C., 2006. Gene expression patterns for GDNF and its receptors in the human putamen affected by Parkinson's disease: a real-time PCR study. Mol. Cell. Endocrinol. 252, 160–166.

Bartus, R.T., Johnson, E.M., 2016a. Clinical tests of neurotrophic factors for human neurodegenerative diseases, part 1: where have we been and what have we learned? Neurobiol. Dis. http://dx.doi.org/10.1016/j.nbd.2016.03.027.

Bartus, R.T., Johnson, E.M., 2016b. Clinical tests of neurotrophic factors for human neurodegenerative diseases, part 2: where do we stand and where must we go next? Neurobiol. Dis. http://dx.doi.org/10.1016/j.nbd.2016.03.026.

Bartus, R.T., Herzog, C.D., Chu, Y., Wilson, A., Brown, L., Siffert, J., Johnson Jr., E.M., Olanow, C.W., Mufson, E.J., Kordower, J.H., 2011. Bioactivity of AAV2-neurturin gene therapy (CERE-120): differences between Parkinson's disease and nonhuman primate brains. Mov. Disord. 26, 27–36.

Bartus, R.T., Baumann, T.L., Brown, L., Kruegel, B.R., Ostrove, J.M., Herzog, C.D., 2013. Advancing neurotrophic factors as treatments for age-related neurodegenerative diseases: developing and demonstrating "clinical proof-of-concept" for AAV-neurturin (CERE-120) in Parkinson's disease. Neurobiol. Aging 34, 35–61.

Bespalov, M.M., Sidorova, Y.A., Tumova, S., Ahonen-Bishopp, A., Magalhães, A.C., Kulesskiy, E., Paveliev, M., Rivera, C., Rauvala, H., Saarma, M., 2011. Heparan sulfate proteoglycan syndecan-3 is a novel receptor for GDNF, neurturin, and artemin. J. Cell Biol. 192, 153–169.

Cacalano, G., Fariñas, I., Wang, L.C., Hagler, K., Forgie, A., Moore, M., Armanini, M., Phillips, H., Ryan, A.M., Reichardt, L.F., Hynes, M., Davies, A., Rosenthal, A., 1998. GFRalpha1 is an essential receptor component for GDNF in the developing nervous system and kidney. Neuron 21, 53–62.

Cardin, A.D., Weintraub, H.J., 1989. Molecular modeling of protein-glycosaminoglycan interactions. Arteriosclerosis 9, 21–32.

Cik, M., Masure, S., Lesage, A.S., Van Der Linden, I., Van Gompel, P., Pangalos, M.N., Gordon, R.D., Leysen, J.E., 2000. Binding of GDNF and neurturin to human GDNF family receptor α 1 and 2. Influence of cRET and cooperative interactions. J. Biol. Chem. 275, 27505–27512.

Davies, J.A., Millar, C.B., Johnson Jr., E.M., Milbrandt, J., 1999. Neurturin: an autocrine regulator of renal collecting duct development. Dev. Genet. 24, 284–292.

Delacoux, F., Fichard, A., Cogne, S., Garrone, R., Ruggiero, F., 2000. Unraveling the amino acid sequence crucial for heparin binding to collagen V. J. Biol. Chem. 275, 29377–29382.

Eigenbrot, C., Gerber, N., 1997. X-ray structure of glial cell-derived neurotrophic factor at 1.9 Å resolution and implications for receptor binding. Nat. Struct. Biol. 4, 435–438.
Fjord-Larsen, L., Johansen, J.L., Kusk, P., Tornøe, J., Grønborg, M., Rosenblad, C., Wahlberg, L.U., 2005. Efficient in vivo protection of nigral dopaminergic neurons by lentiviral gene transfer of a modified neurturin construct. Exp. Neurol. 195, 49–60.
Gash, D.M., Zhang, Z., Ai, Y., Grondin, R., Coffey, R., Gerhardt, G.A., 2005. Trophic factor distribution predicts functional recovery in parkinsonian monkeys. Ann. Neurol. 58, 224–233.
Gill, S.S., Patel, N.K., Hotton, G.R., O'Sullivan, K., McCarter, R., Bunnage, M., Brooks, D.J., Svendsen, C.N., Heywood, P., 2003. Direct brain infusion of glial cell line-derived neurotrophic factor in Parkinson disease. Nat. Med. 9, 589–595.
Golden, J.P., DeMaro, J.A., Osborne, P.A., Milbrandt, J., Johnson Jr., E.M., 1999. Expression of neurturin, GDNF, and GDNF family-receptor mRNA in the developing and mature mouse. Exp. Neurol. 158, 504–528.
Hamilton, J.F., Morrison, P.F., Chen, M.Y., Harvey-White, J., Pernaute, R.S., Phillips, H., Oldfield, E., Bankiewicz, K.S., 2001. Heparin coinfusion during convection-enhanced delivery (CED) increases the distribution of the glial-derived neurotrophic factor (GDNF) ligand family in rat striatum and enhances the pharmacological activity of neurturin. Exp. Neurol. 168, 155–161.
Hoane, M.R., Puri, K.D., Xu, L., Stabila, P.F., Zhao, H., Gulwadi, A.G., Phillips, H.S., Devaux, B., Lindner, M.D., Tao, W., 2000. Mammalian-cell-produced neurturin (NTN) is more potent than purified *Escherichia coli*-produced NTN. Exp. Neurol. 162, 189–193.
Horger, B.A., Nishimura, M.C., Armanini, M.P., Wang, L.C., Poulsen, K.T., Rosenblad, C., Kirik, D., Moffat, B., Simmons, L., Johnson Jr., E., Milbrandt, J., Rosenthal, A., Björklund, A., Vandlen, R.A., Hynes, M.A., Phillips, H.S., 1998. Neurturin exerts potent actions on survival and function of midbrain dopaminergic neurons. J. Neurosci. 18, 4929–4937.
Kirik, D., Rosenblad, C., Björklund, A., Mandel, R.J., 2000. Long-term rAAV-mediated gene transfer of GDNF in the rat Parkinson's model: intrastriatal but not intranigral transduction promotes functional regeneration in the lesioned nigrostriatal system. J. Neurosci. 20, 4686–4700.
Kordower, J.H., Björklund, A., 2013. Trophic factor gene therapy for Parkinson's disease. Mov. Disord. 28, 96–109.
Kotzbauer, P.T., Lampe, P.A., Heuckeroth, R.O., Golden, J.P., Creedon, D.J., Johnson Jr., E.M., Milbrandt, J., 1996. Neurturin, a relative of glial-cell-line-derived neurotrophic factor. Nature 384, 467–470.
Lang, A.E., Gil, S., Patel, N.K., Lozano, A., Nutt, J.G., Penn, R., Brooks, D.J., Hotton, G., Moro, E., Heywood, P., Brodsky, M.A., Burchiel, K., Kelly, P., Dalvi, A., Scott, B., Stacy, M., Turner, D., Wooten, V.G., Elias, W.J., Laws, E.R., Dhawan, V., Stoessl, A.J., Matcham, J., Coffey, R.J., Traub, M., 2006. Randomized controlled trial of intraputamenal glial cell line-derived neurotrophic factor infusion in Parkinson disease. Ann. Neurol. 59, 459–466.
Lin, L.F., Doherty, D.H., Lile, J.D., Bektesh, S., Collins, F., 1993. GDNF: a glial cell line-derived neurotrophic factor for midbrain dopaminergic neurons. Science 260, 1130–1132.
Marks Jr., W.J., Bartus, R.T., Siffert, J., Davis, S.C., Lozano, A., Boulis, N., Vitek, J., Stacy, M., Turner, D., Verhagen, L., Bakay, R., Watts, R., Guthrie, B., Jankovic, J., Simpson, R., Tagliati, M., Alterman, R., Stern, M., Baltuch, G., Starr, P.A., Larson, P.S., Ostrem, J.L., Nutt, J., Kieburtz, K., Kordower, J.H., Olanow, C.W., 2010. Gene delivery of AAV2-neurturin for Parkinson's disease: a double-blind, randomised, controlled trial. Lancet Neurol. 9, 1164–1172.
Parkash, V., Leppänen, V.M., Virtanen, H., Jurvansuu, J.M., Bespalov, M.M., Sidorova, Y.A., Runeberg-Roos, P., Saarma, M., Goldman, A., 2008. The structure of the glial cell line-derived neurotrophic factor-coreceptor complex: insights into RET signaling and heparin binding. J. Biol. Chem. 283, 35164–35172.
Piccinini, E., Kalkkinen, N., Saarma, M., Runeberg-Roos, P., 2013. Glial cell line-derived neurotrophic factor: characterization of mammalian posttranslational modifications. Ann. Med. 45, 66–73.
Planken, A., Porokuokka, L.L., Hänninen, A.L., Tuominen, R.K., Andressoo, J.O., 2010. Medium-throughput computer aided micro-island method to assay embryonic dopaminergic neuron cultures in vitro. J. Neurosci. Methods 194, 122–131.
Rickard, S.M., Mummery, R.S., Mulloy, B., Rider, C.C., 2003. The binding of human glial cell line-derived neurotrophic factor to heparin and heparan sulfate: importance of 2-O-sulfate groups and effect on its interaction with its receptor, GFRalpha1. Glycobiology 13, 419–426.
Runeberg-Roos, P., Saarma, M., 2007. Neurotrophic factor receptor RET: structure, cell biology, inherited diseases. Ann. Med. 39, 572–580.
Sainio, K., Suvanto, P., Davies, J., Wartiovaara, K., Saarma, M., Arumäe, U., Meng, X., Lindahl, M., Pachnis, V., Sariola, H., 1997. Glial-cell-line-derived neurotrophic factor is required for bud initiation from ureteric epithelium. Development 124, 4077–4087.
Salvatore, M.F., Ai, Y., Fischer, B., Zhang, A.M., Grondin, R.C., Zhang, Z., Gerhardt, G.A., Gash, D.M., 2006. Point source concentration of GDNF may explain failure of phase II clinical trial. Exp. Neurol. 202, 497–505.
Slevin, J.T., Gerhardt, G.A., Smith, C.D., Gash, D.M., Kryscio, R., Young, B., 2005. Improvement of bilateral motor functions in patients with Parkinson disease through the unilateral intraputaminal infusion of glial cell line-derived neurotrophic factor. J. Neurosurg. 102, 216–222.
Timmusk, T., Belluardo, N., Metsis, M., Persson, H., 1993. Widespread and developmentally regulated expression of neurotrophin-4 mRNA in rat brain and peripheral tissues. Eur. J. Neurosci. 5, 605–613.
Virtanen, H., Yang, J., Bespalov, M.M., Hiltunen, J.O., Leppänen, V.M., Kalkkinen, N., Goldman, A., Saarma, M., Runeberg-Roos, P., 2005. The first cysteine-rich domain of the receptor GFRalpha1 stabilizes the binding of GDNF. Biochem. J. 387, 817–824.
Voutilainen, M.H., Bäck, S., Pörsti, E., Toppinen, L., Lindgren, L., Lindholm, P., Peränen, J., Saarma, M., Tuominen, R.K., 2009. Mesencephalic astrocyte-derived neurotrophic factor is neurorestorative in rat model of Parkinson's disease. J. Neurosci. 29, 9651–9659.
Yin, D., Valles, F.E., Fiandaca, M.S., Forsayeth, J., Larson, P., Starr, P., Bankiewicz, K.S., 2009. Striatal volume differences between non-human and human primates. J. Neurosci. Methods 176, 200–205.